

## Geomechanical parameters in the active zone of an unsaturated tropical soil site via laboratory tests

Jeferson Brito Fernandes<sup>1</sup> , Alfredo Lopes Saab<sup>1</sup> , Breno Padovezi Rocha<sup>2#</sup> ,  
Roger Augusto Rodrigues<sup>1</sup> , Paulo César Lodi<sup>1</sup> , Heraldo Luiz Giacheti<sup>1</sup> 

Article

### Keywords

Unsaturated soil  
Suction  
Triaxial compression test  
Bender elements  
Oedometer test

### Abstract

The seasonal variability of geotechnical parameters in the unsaturated zone is typically neglected in the design of geotechnical works. In most of the geotechnical projects the parameters are determined only for the saturated condition. Although it is known that this condition is the most critical to soil strength and deformability, this conservative approach may neglect a possible important contribution of the unsaturated condition, resulting in an increase in the cost of the geotechnical solution. This paper presents and discusses the site characterization of the active zone of an unsaturated sandy soil profile under different suction conditions. Laboratory tests with controlled suction (retention curves, triaxial compression with bender elements and oedometer tests) were carried out on undisturbed samples collected from 1.0 to 5.0 m depth. The results show that strength and deformability parameters are strongly affected by soil suction and are less influenced by confinement stress up to 5.0 m depth. All the investigated subsoil profile shows a collapsible behavior, more pronounced closer to the ground surface and under the effect of higher suction values. The findings highlight the importance of incorporating the suction influence in the site investigation, parameter determination, and geotechnical design for more economical, reliable, and environmentally sustainable solutions.

## 1. Introduction

Urban growth contributes to an increase in regional temperatures, alters the rainfall regime, and causes local extreme events and natural disasters. Southeastern Brazil is one of the regions where there is a greater tendency for precipitation increase, while in the Northeast there is drought. It is important to advance the understanding of the geomechanical behavior of soils in tropical and subtropical climatic environments by studying key aspects that are not yet well understood, such as the impact of the unsaturated state on the laboratory and in situ determination of the geomechanical properties of these soils (Vilar & Rodrigues, 2011; Zhang et al., 2014; Zhang, 2016). This aspect is also important in the design of infrastructure works with emphasis on the seasonal variability that may occur (Fernandes, 2016; Dong et al., 2018; Silva et al., 2019).

The behavior of unsaturated soils depends on the moisture content and consequently on the soil suction. Changes in the moisture content and suction in an unsaturated soil can occur due to climate variations (Blight, 2003; Cui et al., 2005).

It is important to know the soil properties through direct in situ or laboratory measurements in the geotechnical design practice. The time of year when a particular unsaturated soil site is investigated can have a strong influence mainly on the in-situ test data (Giacheti et al., 2019; Rocha et al., 2021).

The depth of the subsoil to which changes in moisture content take place is referred to as the active zone. The active zone is generally defined as the region of fluctuation in moisture content of an unsaturated soil, which can change seasonally due to climatic variations (Fredlund, 2006). Significant soil deformation or movement can occur due to variations in soil moisture/energy in this zone. It is important to note that varying soil suction affects the behavior of collapsible and expansive unsaturated soils. Lightweight structures such as highways and railroads (Sánchez et al., 2014) or small buildings are often subject to severe damage due to wetting of a collapsible or expansive soil. Abrupt and significant settlements in geotechnical structures are common in collapsible soils after flooding (Jennings & Knight, 1975; Vilar & Rodrigues, 2011). Cut slopes (Tsiampousi et al., 2017) and infinite slopes (Ray et al., 2010; Zhang et al., 2014) are

#Corresponding author. E-mail address: breno.rocha@ifsp.edu.br.

<sup>1</sup>Universidade Estadual Paulista "Júlio de Mesquita Filho", Faculdade de Engenharia, Departamento de Engenharia Civil e Ambiental, Bauru, SP, Brasil.

<sup>2</sup>Instituto Federal de São Paulo, Ilha Solteira, SP, Brasil.

Submitted on January 9, 2022; Final Acceptance on October 4, 2022; Discussion open until February 28, 2023.

<https://doi.org/10.28927/SR.2022.000422>



This is an Open Access article distributed under the terms of the Creative Commons Attribution License, which permits unrestricted use, distribution, and reproduction in any medium, provided the original work is properly cited.

prone to rupture or may experience irreversible movement due to changes in negative soil and water pressures. Therefore, seasonal variability can lead to complex and often costly assessment of unsaturated soil properties, from a practical point of view. However, even today, geotechnical designs rely almost exclusively on data obtained through short-term site investigation programs.

The conventional laboratory tests, i.e., those that are performed without any soil suction control, generally do not adequately consider the transient condition of moisture content. Modern laboratory testing options are available (Delage et al., 2008) to consider the suction influence on soil behavior. It is important to recognize the significant progress that suction control has brought to the understanding of unsaturated soils, especially Hilf's (1956) axis translation technique.

Some researchers in recent decades have proposed ways to interpret laboratory test data on unsaturated soils. It has been usual to consider two independent stress state variables (suction and net stress) over a wide suction range (Fredlund & Morgenstern, 1977; Toll, 1990). It can range from 0 to 500 kPa for most geotechnical engineering problems, according to (Khalili & Khabbaz, 1998; Vanapalli et al., 1996). Fredlund et al. (1978) and Ho & Fredlund (1982) extended the Mohr-Coulomb criterion for unsaturated soils using state variables by defining failure surfaces assumed as planar and represented by friction angles  $\phi'$  and  $\phi^B$ .

Escario & Sáez (1986) found the non-linearity of  $\phi^B$  from the interpretation of experimental data and it prompted some researchers to propose empirical models to represent the total cohesion intercept (e.g., Vanapalli et al., 1996; Vilar, 2006). The failure envelopes of unsaturated soils can be determined in laboratory via triaxial compression tests with controlled suction (Fredlund et al., 1978; Khalili & Khabbaz, 1998; Vanapalli et al., 1996; Zhang, 2016). The drainage conditions in the consolidation and shear phase can be different depending on the type of triaxial test performed.

Modern triaxial compression testing devices allow to use equipment for the direct measurement of load and displacement of soil specimens within the triaxial cells. Bender elements have also been used to measure shear wave velocities ( $V_s$ ) with deformations in the order of  $10^{-4}$  to  $10^{-6}\%$ . Therefore, theory of elasticity is valid to determine the maximum shear modulus ( $G_0$ ):

$$G_0 = \rho \cdot V_s^2 \quad (1)$$

$G_0$  is a reference geotechnical parameter to be considered in the site characterization for geotechnical design (Jamiolkowski, 2012; Rocha et al., 2022). The triaxial compression test system equipped with bender elements allow to verify the quality of specimen (Ferreira et al., 2011). It also allows determining the variation of  $G_0$  with the confining net stress, void ratio, soil suction, and over consolidation ratio (Dong et al., 2018; Dong & Lu, 2016; Georgetti, 2014; Hardin & Blandford, 1989; Hoyos et al., 2015; Leong & Cheng, 2016; Nyunt et al., 2011).

The compressibility parameters are also important in a proper site characterization program, especially for foundation settlements prediction (Skempton & Jones, 1944; Lambe & Whitman, 1976). The compressibility of unsaturated soils, mainly the collapsible ones, is more complex and difficult to predict since suction changes can induce significant variation in compressibility parameters such as the over consolidation stress and the compression index.

Jennings & Knight (1975) proposed the use of single and double oedometer tests since many unsaturated soils present collapsible behavior. Sun et al. (2007) conducted suction-controlled tests on a compacted clay to study the influence of different dry unit weight and suction values on the collapse behavior for both isotropic and anisotropic stress states. Vilar & Rodrigues (2011) carried out suction-controlled tests on an undisturbed clayey sand to study the soil collapsibility with the gradual reduction of suction upon vertical stresses.

The main research goal in the recent years has been to understand the behavior of unsaturated soils extending the concepts of the Critical States Soil Mechanics (Alonso et al., 1990). Research has been based on experimental data in which the axis translation technique is used mainly as a tool to understand the hydraulic and mechanical behavior of unsaturated soils. So, controlled suction laboratory tests are essential to understand the unsaturated soil behavior and its seasonal variability in the active zone of the soil profile.

This paper presents and discusses the characterization via laboratory tests of the active zone of an unsaturated tropical sandy soil profile under different suction conditions. The main contribution is to highlight the importance of incorporating the suction influence on determining soil parameters and considering it in the geotechnical engineering design as well as to expand the database of geotechnical parameters in a typical unsaturated tropical soil.

## 2. Materials and methods

### 2.1 Study site

The study site is the experimental research area (Lat.: S 22°05' to S 22°26'; Long.: W 49°00' to W 49°16') from the São Paulo State University, in Bauru, São Paulo, Brazil. The geology consists predominantly of sediments from Bauru Group (Marília and Adamantina Formations), covering the volcanic rocks of Serra Geral Formation that outcrop towards the Valley of the Tietê River. De Mío (2005) describes these soils as being formed mainly by deposits of colluvial origin submitted to tropical weathering process, resulting in porous and collapsible soils.

Figure 1 shows some index properties and grain size distribution (with and without dispersant) up to 6 m depth. The soil is classified as clayey sand and the grain size distribution is relatively uniform. The dry unit weight ( $\gamma_d$ ) and unit weight of solids ( $\gamma_s = 26.8 \text{ kN/m}^3$ ) are practically

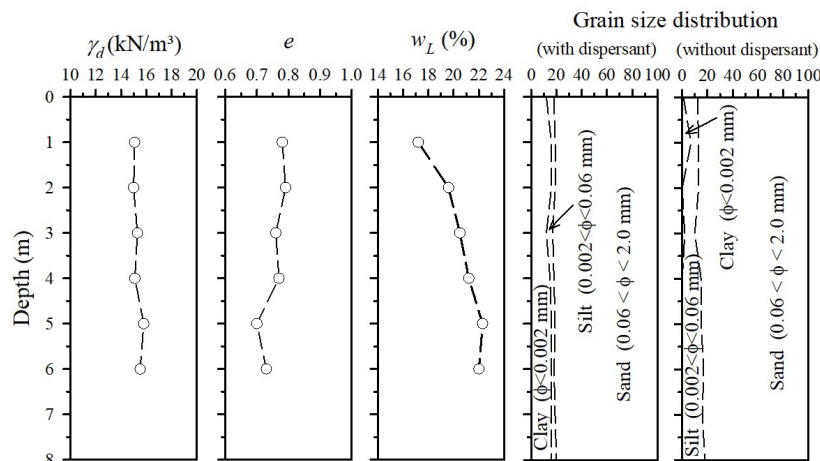


Figure 1. Grain size distribution and index properties [adapted from Giacheti et al. (2019)].

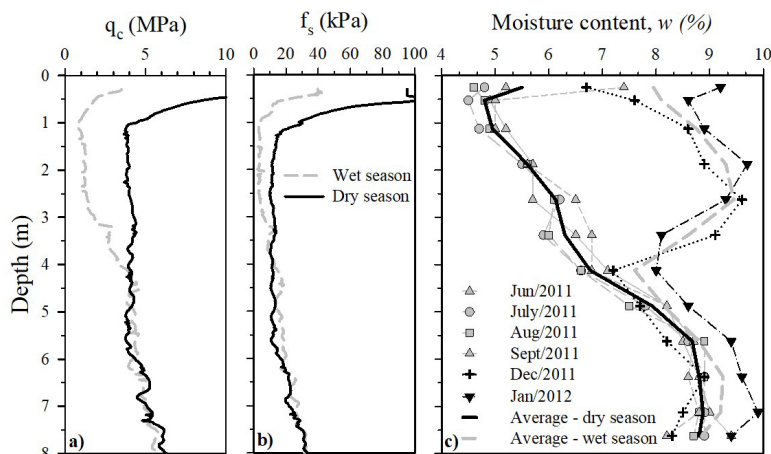


Figure 2. Wet and dry seasons profiles: (a) and (b) average CPT data; (c) moisture content data [adapted from Giacheti et al. (2019)].

constant with depth. The void ratio ( $e$ ) at 1.0 m depth is equal to 0.78 and it is also almost constant up to 4 m depth and drops to about 0.70 at 5 and 6 m depth. The liquid limit at 1.0 m depth ( $w_L$ ) is 17% and tends to increase with depth. The fine portion of the soil is non-plastic (plastic limit -  $w_p$ , cannot be determined) and has iron and aluminum oxides, hydroxides, and kaolinite. It is classified as SM Group soil in the Unified Soil Classification System (ASTM, 2017).

The study site has a tropical climate with well-defined wet and dry seasons. The Cone and the Piezocone Penetration Tests (CPT and CPTu) can be used as a high profiling resolution technique to assess site stratigraphy and variability (De Mio & Giacheti, 2007). Giacheti et al. (2019) investigated the seasonal influence on the study site based on CPT campaigns carried out in different season of the year. The tests were carried out in a wooded area with some *Caesalpinia peltophoroides Benth*, commonly referred as “*Sibipirunas*”. The trees are likely to have a system of lateral roots and one large tap root and affected the seasonal variability.

The role of suction on soil behavior can be observed in Figure 2a, 2b since the seasonal variation has significantly influenced the CPT data up to about 4 to 5 m depth. The monitoring of the moisture content profiles (Figure 2c) indicates that a high variation occurs closer to the ground surface, and it decreases with depth.

## 2.2 Laboratory tests

Soil blocks were retrieved from exploratory sampling pits to get disturbed and undisturbed samples following ABNT (1986). Laboratory tests for soil characterization (physical indexes, grain size distribution and Atterberg limits) were carried out every meter interval up to 5 m depth. Soil water retention curves were determined under drying trajectory by using the filter paper technique, suction plate, and pressure plate tests. The specimens were obtained from quasi-static driving of beveled PVC rings (53 mm in diameter and 12 mm high) on undisturbed samples collected at 1.0, 3.0 and 5.0 m depth. The specimens were saturated with distilled and de-aerated

water. The filter paper *Whatman* n° 42 and the calibration of Chandler & Gutierrez (1986) and Chandler et al. (1992) were used to determine the experimental data points by the filter paper method following the procedures suggested by Marinho & Oliveira (2006). The equation proposed by van Genuchten (1980) was used to adjust experimental datapoints obtained by different methods.

Soil shear strength was determined through saturated and unsaturated consolidated drained triaxial compression tests (CD type) with an axial strain rate of 0.05%/min to endure dissipation of the excess pore water pressure during all tests. Specimens 50 mm in diameter by 100 mm in height were carved from undisturbed soil samples collected at 1.5, 3.0, and 5.0 m depth by an exploratory sample pit. The experimental test program was designed to ensure the integrity of specimens, as well as the quality of the collected samples. The soil suction values were 0, 50, 200, and 400 kPa and the net normal stresses were 50, 100 and 200 kPa. The saturation (zero suction) was achieved applying back pressure up to a pore-pressure coefficient  $B \geq 0.95$ .

Table 1 presents the index properties of the samples before and after saturated and unsaturated triaxial tests.

The suction values were installed in the unsaturated specimens and maintained through Hilf (1956) axis-translation technique by means of a 500 kPa air entry value porous plate. The pore-air pressure was elevated above atmospheric pressure such that pore-water pressure becomes positive (Hilf, 1956; Fredlund, 2006). The failure envelopes Fredlund et al. (1978) were determined for each investigated depth to obtain friction angle and the cohesion intercept (Vilar, 2006).

The maximum shear modulus ( $G_{\theta}$ ) was determined in a triaxial chamber equipped with bender elements. The specimens were carved from the undisturbed samples collected at 1.5, 3.0, and 5.0 m depths. The suction levels were 0, 50, 200 and 400 kPa and isotropic state stresses were 25, 50, 100 and 200 kPa. The shear wave velocity ( $V_s$ ) was determined by the first time of arrival method, after the specimen consolidation (Fernandes, 2016). The  $G_{\theta}$  variations as a function of soil suction and net normal stress were determined for each tested depth.

**Table 1.** Index properties for the soil samples before and after the triaxial tests.

Depth (m)	Net normal stress (kPa)	Index properties	Soil suction, $s$ (kPa)							
			0		50		200		400	
			Before	After	Before	After	Before	After	Before	After
1.5	50	$e$	0.689	0.584	0.710	0.599	0.761	0.705	0.788	0.759
		$w$ (%)	5.10	20.12	6.05	7.00	5.94	6.17	5.65	5.69
		$\gamma_d$ (kN/m <sup>3</sup> )	15.96	17.02	15.77	16.86	15.31	15.82	15.08	15.32
	100	$e$	0.717	0.579	0.749	0.574	0.769	0.668	0.776	0.714
		$w$ (%)	5.82	18.24	5.64	7.05	5.94	6.12	5.79	5.65
		$\gamma_d$ (kN/m <sup>3</sup> )	15.70	17.07	15.41	17.13	15.24	16.16	15.18	15.73
	200	$e$	0.703	0.409	0.711	0.532	0.781	0.628	0.807	0.608
		$w$ (%)	5.71	19.36	5.90	7.15	5.42	6.07	5.92	*
		$\gamma_d$ (kN/m <sup>3</sup> )	15.83	18.09	15.76	17.61	15.14	16.56	14.92	16.76
3.0	50	$e$	0.814	0.665	0.742	0.690	0.741	0.706	0.726	0.709
		$w$ (%)	8.35	*	8.31	*	7.88	6.97	7.25	6.43
		$\gamma_d$ (kN/m <sup>3</sup> )	14.79	16.11	15.40	15.88	15.41	15.73	15.54	15.70
	100	$e$	0.740	0.566	0.748	0.641	0.734	0.665	0.770	0.703
		$w$ (%)	8.08	*	8.29	*	8.62	6.59	8.64	6.55
		$\gamma_d$ (kN/m <sup>3</sup> )	15.42	17.13	15.35	16.35	15.47	16.12	15.16	15.76
	200	$e$	0.753	0.534	0.745	0.653	0.733	0.605	0.791	0.608
		$w$ (%)	8.61	*	7.85	*	7.61	6.31	9.19	7.07
		$\gamma_d$ (kN/m <sup>3</sup> )	15.31	17.49	15.38	16.24	15.48	16.72	14.98	16.68
5.0	50	$e$	0.717	0.605	0.674	0.654	0.688	0.671	0.702	0.678
		$w$ (%)	10.23	*	10.27	7.93	9.12	7.78	9.84	7.23
		$\gamma_d$ (kN/m <sup>3</sup> )	15.67	16.76	16.07	16.26	15.94	16.10	15.80	16.03
	100	$e$	0.684	0.532	0.697	0.598	0.692	0.646	0.697	0.663
		$w$ (%)	10.54	*	10.22	8.10	8.93	7.11	9.01	7.15
		$\gamma_d$ (kN/m <sup>3</sup> )	15.97	17.55	15.85	16.83	15.90	16.34	15.85	16.18
	200	$e$	0.712	0.537	0.707	0.621	0.704	0.602	0.686	0.607
		$w$ (%)	10.31	*	10.05	8.25	9.98	7.18	9.86	6.98
		$\gamma_d$ (kN/m <sup>3</sup> )	15.71	17.50	15.76	16.59	15.79	16.79	15.95	16.74

\*Not determined.

Conventional and controlled-suction oedometer tests were performed using oedometer-type chambers like the one developed by Escario & Sáez (1986). The compressibility parameters for the undisturbed soil samples collected at 1.0, 2.0, 3.0, 4.0 and 5.0 m depth were determined under different suction values (0, 50, 100, 200 and 400 kPa).

The specimens were retrieved from a quasi-static driving of a metal ring of 70 mm diameter and 25 mm high. They were inundated with distilled and deaired water and installed on high air-entry porous plate at the base of the oedometer-type chambers. The specimens were subjected to air pressure inside the chamber, which allowed the imposition of suction through axis-translation technique of Hilf (1956). A total of 25 confined compression curves were determined for 5 different soil suction values (0, 50, 100, 200 and 400 kPa) and for each test depth (from 1.0 to 5.0 m). Table 2 presents the index properties of the samples before and after oedometer tests.

### 3. Analysis and results

#### 3.1 Soil water retention curve

Figure 3 shows the experimental data, in terms of gravimetric moisture content ( $w$ ) and soil suction ( $s$ ), as well as the best curves fitted for 1.0, 3.0 and 5.0 m depth samples. All the curves are typical of sandy soils with low water retention (Fredlund & Xing, 1994). They are bimodal with four zones: a boundary effect zone, two transition zones and a residual zone (Vanapalli et al., 1996). The boundary effect zone is short, from 0 to 2 kPa in which the soil is saturated by capillarity. The transition zones start from the point of the first air entry

value (AEV), about 2 kPa, ending at the residual moisture, around 2%. As the suction increases the moisture decreases significantly in the transition zones. Values of soil suction higher than the first air entry value (about 2 kPa) and lower than the second air entry value (about 1 MPa), indicate that the macropores and soil micropores are respectively unsaturated and saturated. The water in the micropores begins to drain significantly for suction values between the second air entry value and the residual moisture content. A large variation on suction causes a little change in moisture content in the residual zone. The soil pores are occupied mainly by air and the liquid phase is discontinuous in this zone.

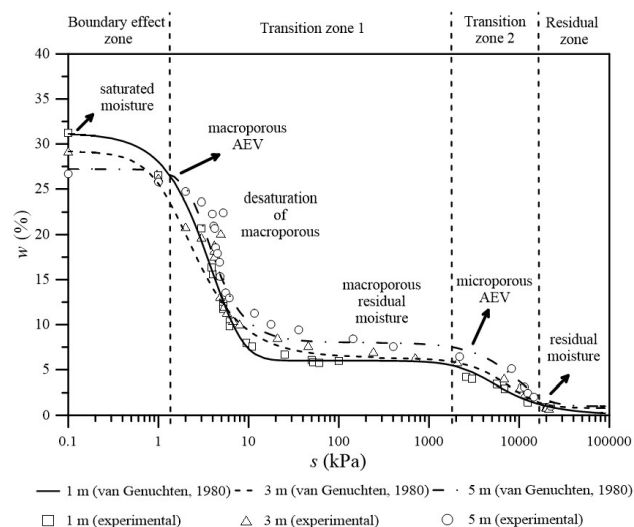


Figure 3. Soil water retention curves for the collect soil samples.

Table 2. Index properties for the soil samples before and after the oedometer tests.

Depth (m)	Index properties	Soil suction, $s$ (kPa)									
		0		50		100		200		400	
		Before	After	Before	After	Before	After	Before	After	Before	After
1.0	$e$	0.849	0.477	0.856	0.554	0.853	0.544	0.841	0.587	0.811	0.612
	$w$ (%)	8.06	18.21	7.87	7.16	7.87	6.89	7.89	6.15	8.15	5.94
	$\gamma_d$ (kN/m <sup>3</sup> )	14.58	18.25	14.53	17.35	14.55	17.46	14.64	16.99	14.89	16.72
2.0	$e$	0.871	0.500	0.889	0.569	0.959	0.586	0.907	0.619	0.806	0.610
	$w$ (%)	9.3	19.35	9.30	8.27	9.53	7.83	9.65	7.28	9.65	7.19
	$\gamma_d$ (kN/m <sup>3</sup> )	14.60	17.89	14.24	17.18	13.73	17.00	14.11	16.65	14.89	16.75
3.0	$e$	0.838	0.500	0.776	0.523	0.769	0.528	0.663	0.519	0.744	0.545
	$w$ (%)	7.57	19.9	9.07	8.46	9.07	7.34	9.11	7.05	9.11	6.95
	$\gamma_d$ (kN/m <sup>3</sup> )	14.60	17.89	15.11	17.62	15.17	17.56	16.13	17.66	15.39	17.37
4.0	$e$	0.816	0.497	0.827	0.544	0.794	0.551	0.732	0.560	0.791	0.607
	$w$ (%)	8.74	21.04	9.10	8.48	9.10	8.21	8.76	7.33	8.76	7.16
	$\gamma_d$ (kN/m <sup>3</sup> )	14.81	17.97	14.72	17.42	14.99	17.34	15.53	17.24	15.02	16.74
5.0	$e$	0.765	0.496	0.703	0.504	0.718	0.542	0.730	0.555	0.737	0.565
	$w$ (%)	10.25	18.36	10.30	9.19	10.11	8.19	10.15	7.79	9.83	7.61
	$\gamma_d$ (kN/m <sup>3</sup> )	15.24	18.02	15.80	17.93	15.66	17.48	15.55	17.34	15.49	17.23

### 3.2 Shear strength

Figures 4 show the triaxial compression tests data in terms of the variation of deviatoric stress *versus* axial strain and variation of volumetric strain *versus* axial strain.

There is no clear peak stress in the curves independently of the test depth and soil suction (Figure 4). After reaching a

certain stress value, the strain increases almost continuously with no increase in stress. It shows a contractive behavior during shearing, as can be seen in the volumetric strain *versus* axial strain curves (Figure 4).

The interpretation of the data presented in Figure 4 indicates a slight increase of soil rigidity with increasing depth and soil suction, as can be seen in Figure 5 in terms of the secant

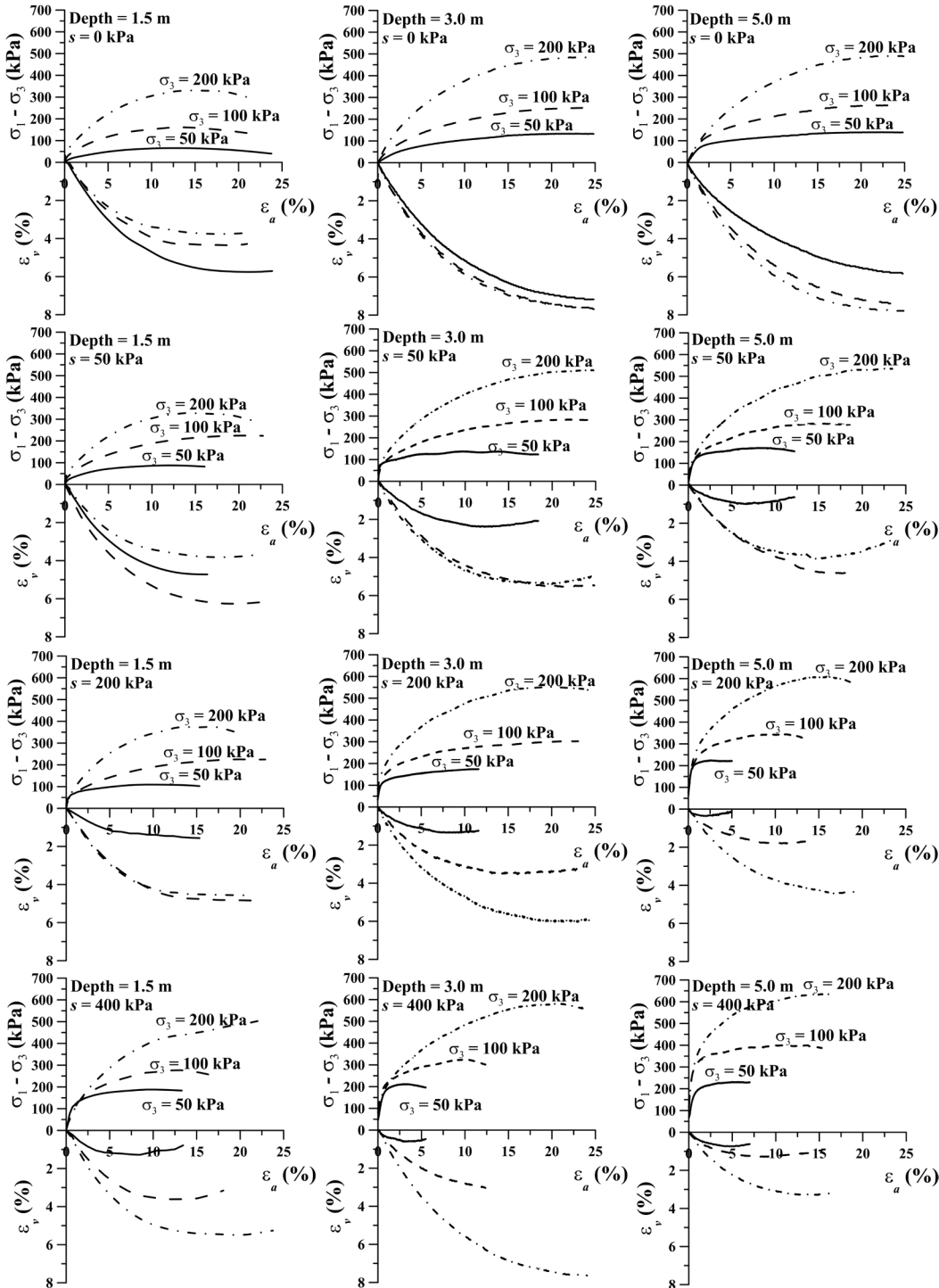


**Figure 4.** Variation of deviatoric stress *versus* axial strain and variation of volumetric strain *versus* axial strain for the triaxial compression tests. Data for different depths and soil suctions.

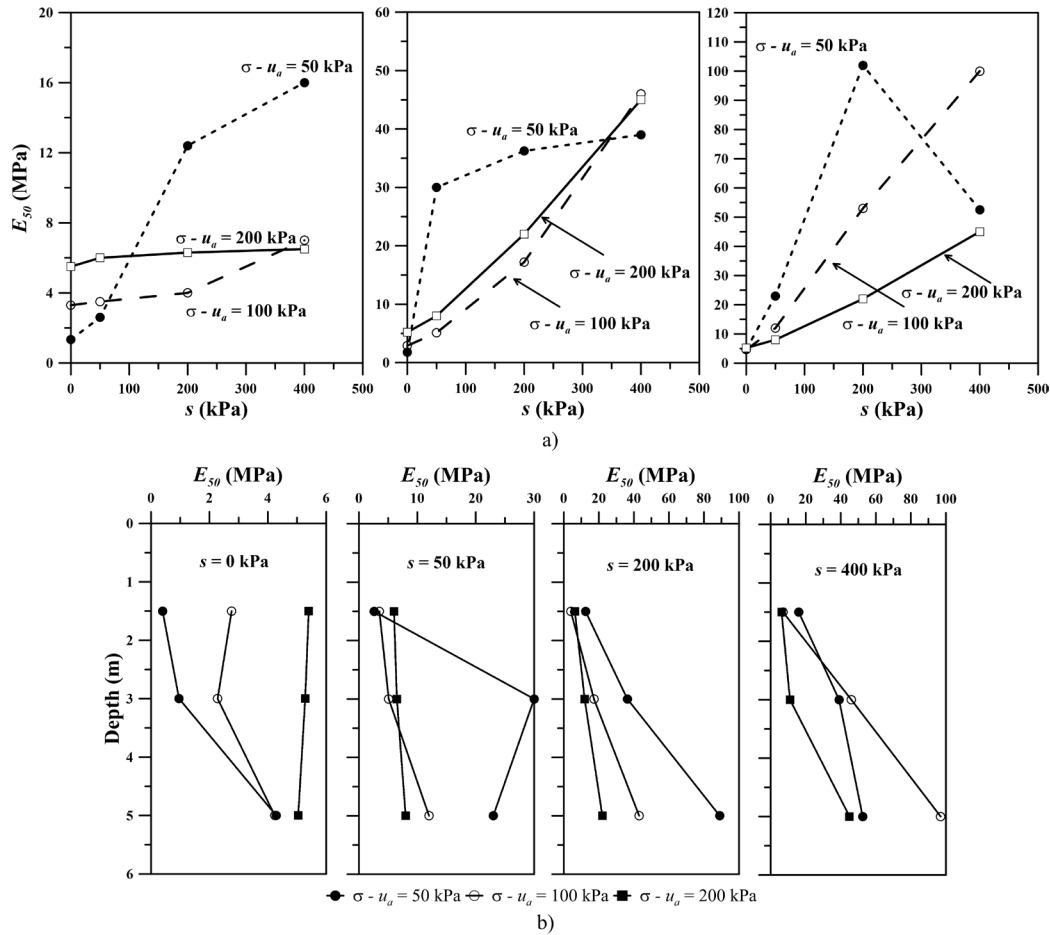


Figure 5. Variation of secant modulus ( $E_{50}$ ) with (a) soil suction and (b) depth.

modulus in drained triaxial testing at 50 percent strength ( $E_{50}$ ). Such behavior is mainly related to the increase of the over consolidation stress with depth and soil suction, which is going to be presented and discussed later, based on the confined compression test data.

The Mohr-Coulomb failure envelopes from Figure 6 were defined after the interpretation of the deviatoric stress curves versus axial strain for the three different depths. They were defined after the interpretation of the deviatoric stress curves *versus* axial strain for the three different sample depths (Figure 4). The maximum deviatoric stress ( $\sigma_1 - \sigma_3$ )<sub>max</sub> was used as the failure criterion. The envelopes were drawn by fitting a straight-line tangent to the three Mohr failure circles drawn from the interpretation of the data from each series of tests, depending on the test depth and soil suction.

The failure envelopes indicate that there are differences between saturated and unsaturated soils mainly in terms of the cohesion intercepts (Figure 7). The soil from 1.5 m depth has a cohesion intercept that varies from 0 to 16 kPa while the soil at the 5 m depth varies from 5.3 to 28.7 kPa. It can also be seen in this figure that the inclinations of shear strength failure envelope for 3 and 5 m depth samples are

approximately equal regardless of the suction values. This means that the internal friction angle of the soil shows little changes with suction to higher depths. It is interesting to point out that grain size distribution of these soils is almost the same along depth (Figure 1).

The friction angle varies little with suction and the cohesion intercept increases hyperbolically with suction. The hyperbolic fit Equation 2 is shown in Figure 7, which led to coefficients of determination ( $R^2$ ) close to the unit. Table 3 shows the values of constants  $a$  and  $b$  from the hyperbolic equation representative for each tested depth. Such behavior was observed by (Escario & Sáez, 1986; Röhm & Vilar, 1995; Vilar, 2006).

$$\tau = c' + (\sigma - u_a) \cdot \text{tg } \Phi' + s \cdot \frac{1}{a + b \cdot s} \quad (2)$$

### 3.3 Maximum shear modulus

The  $G_0$  values determined in the laboratory using bender elements is presented in Figure 8. It can be seen in this figure that  $G_0$  tends to increase linearly with net confining stress

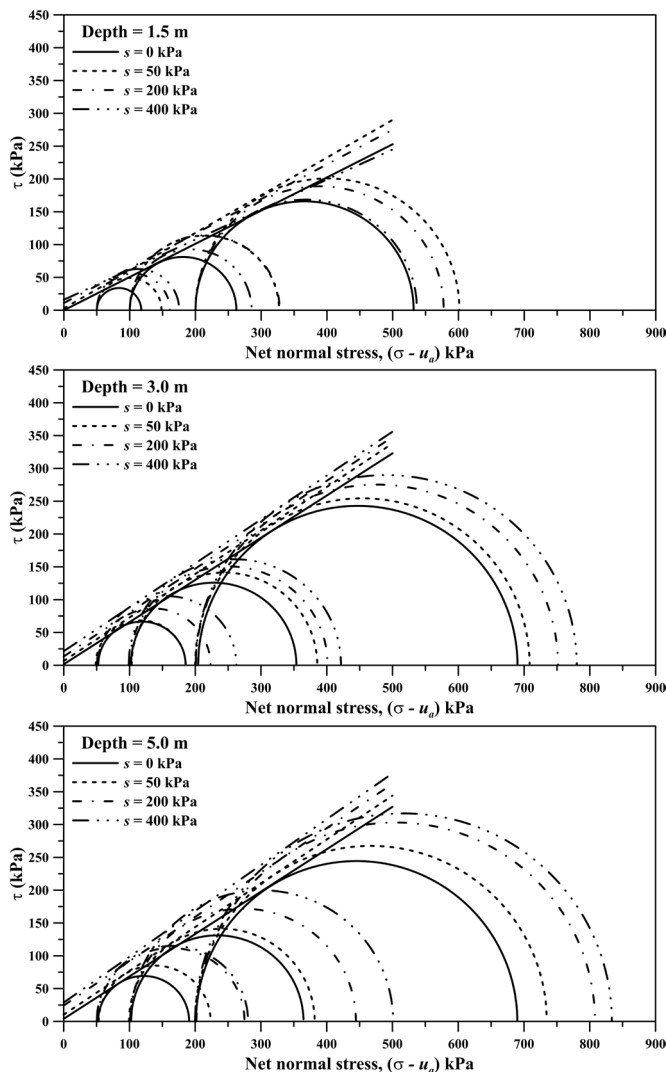


Figure 6. CD controlled suction triaxial compression test failure envelopes for different sample depth and soil suction values.

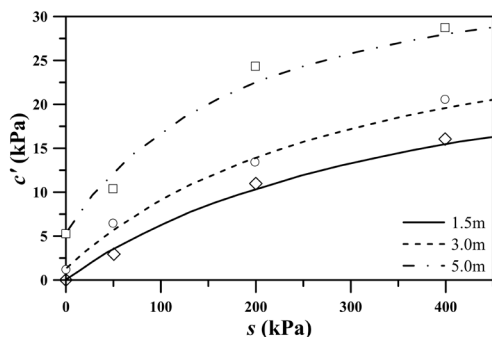


Figure 7. Cohesion intercept versus soil suction for different test depth and the hyperbolic fit.

Table 3. Values of  $c'$  and  $\phi'$ , fitting parameters ( $a$  and  $b$ ) and coefficient of determination ( $R^2$ ).

Depth (m)	$c'$ (kPa)	$\phi'$ (°)	$a$	$b$	$R^2$
1.5	0.0	26.8	12.5	0.032	1.00
3.0	1.2	32.6	9.5	0.029	0.99
5.0	5.3	32.4	5.6	0.029	0.98

and nonlinearly with soil suction for the three tested depths. The same behavior (i.e., nonlinearity between  $G_0$  and soil suction and linearity between  $G_0$  and net confining stress) was also observed for unsaturated reconstituted sands by Nyunt et al. (2011) using, however, different equations to represent these behaviors. To better represent the influence of net stress and soil suction on soil stiffness, Equation 3 and Equation 4 were respectively used to fit the experimental data.

$$G_0 = f + g \cdot (\sigma - u_a) \tag{3}$$

$$G_0 = G_{0,sat} + \frac{s}{m + (n \cdot s)} \tag{4}$$

Where  $G_0$  is the maximum shear modulus at the saturated condition,  $(\sigma - u_a)$  is the net confining stress,  $s$  is the soil suction, and  $f, g, m,$  and  $n$  are the fitting parameters.

Table 4 shows the fitting parameters for  $G_0$  and net confining stress and Table 5 the fitting parameters for  $G_0$  and soil suction for the 1.5 m depth sample.

**Table 4.** Values of the fitting parameters for the sample collected at 1.5 m depth to represent the variation of  $G_0$  with net stress.

$u_a - u_w$ (kPa)	$f$	$g$	$R^2$
0	40.7	0.5502	0.99
50	64.0	0.5413	0.99
200	70.5	0.5979	0.99
400	74.4	0.6055	0.99

**Table 5.** Values of the fitting parameters for the sample collected at 1.5 m depth to represent the variation of  $G_0$  with soil suction.

$\sigma - u_a$ (kPa)	$m$	$n$	$R^2$
25	0.8068	0.0294	0.99
50	0.7279	0.0226	1.00
100	1.3801	0.0238	0.99
200	1.0835	0.0194	0.99

Figure 8 also shows an increase of  $G_0$  with the test depth (i.e., net confining stress) and that  $G_0$  increased at a faster rate with soil suction, up to approximately 50 kPa. In general,  $G_0$  tend to increase with soil suction and net confining stress. Such behavior is attributed to an increase in soil stiffness (higher rigidity of soil skeleton) due to either soil suction or confining pressure (Leong et al., 2006; Mancuso et al., 2002; Takkabutr, 2006).

### 3.4 Compressibility

Figure 9 shows the confined compression curves determined by the oedometer tests carried out with constant suction value for all the test depths. The data interpretation shows an increase on stiffness with increasing suction. It can also be seen in this figure that over consolidation

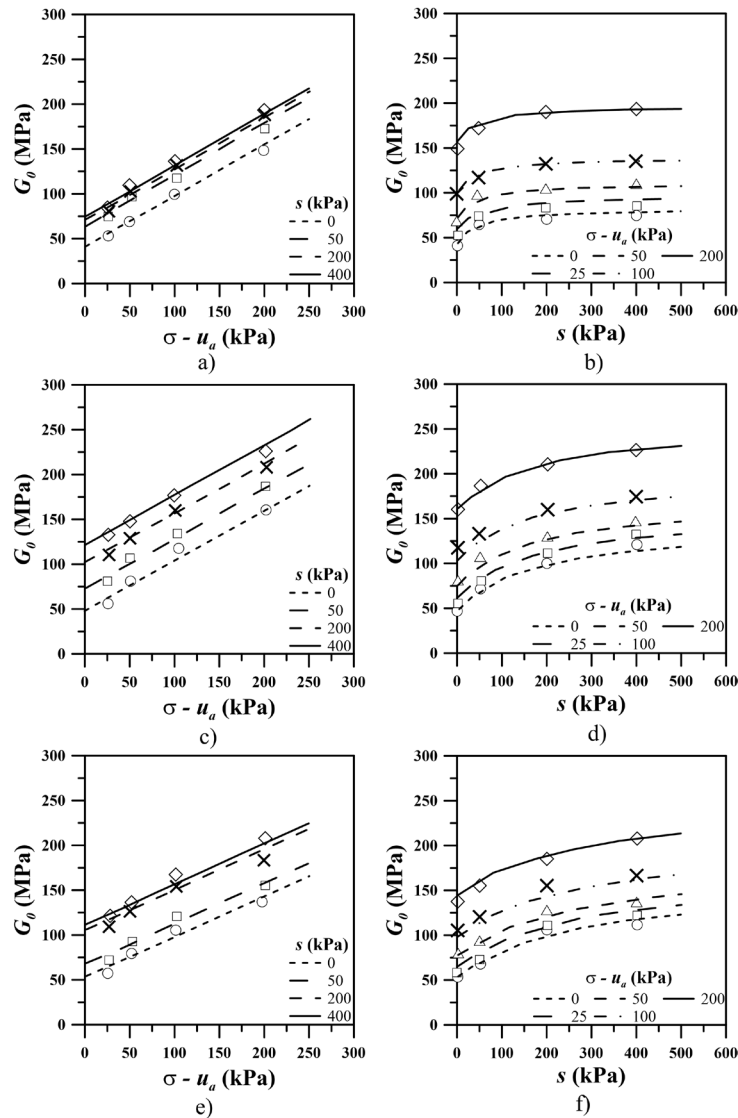


**Figure 8.** Variation of maximum shear modulus with net stress (a, c, and e) and soil suction (b, d, and f) as well as the fitting equations for samples collected at 1.5, 3.0 and 5.0 m depth.

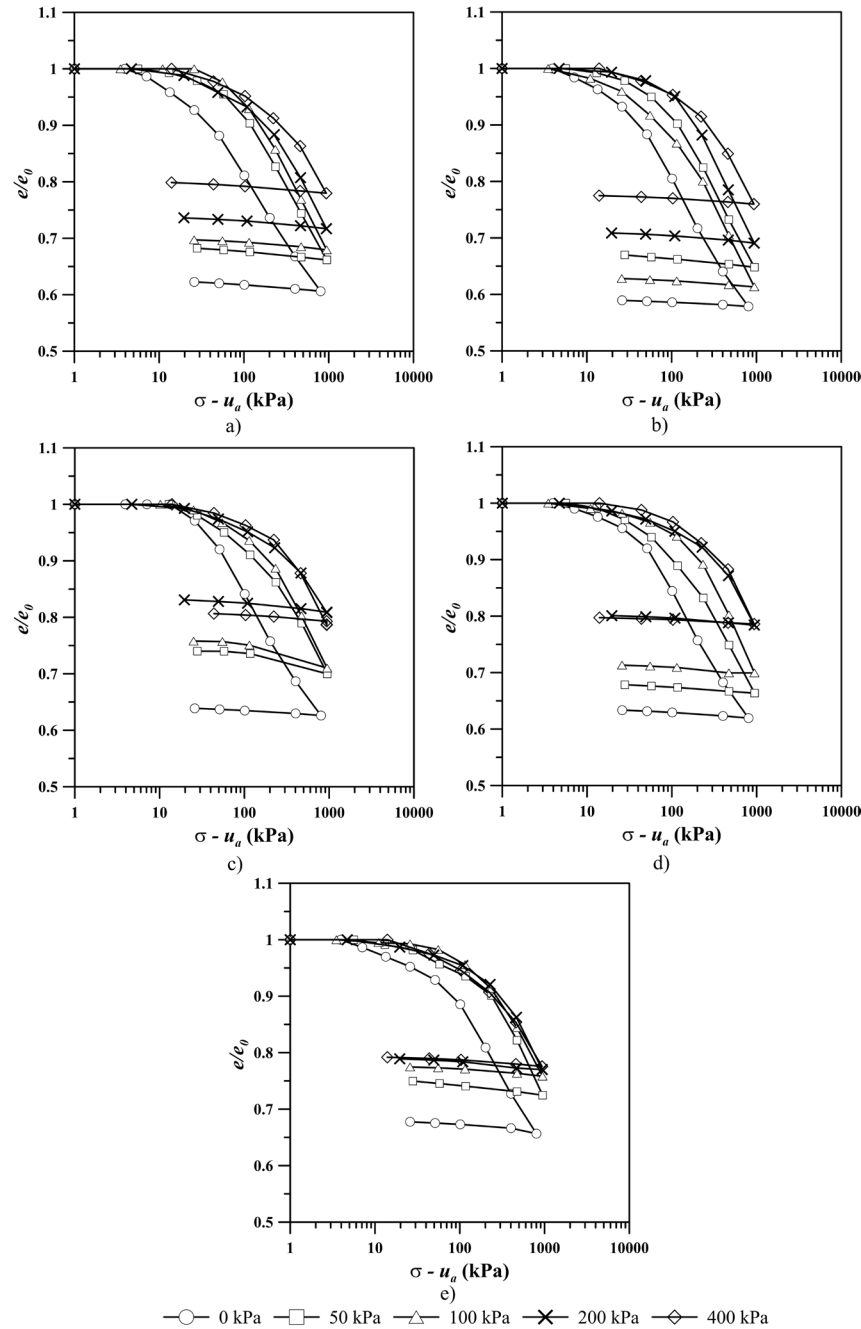


**Figure 9.** Controlled suction oedometer test data determined for soil samples collected at (a) 1.0; (b) 2.0; (c) 3.0; (d) 4.0; and (e) 5.0 m depth.

stress ( $\sigma_p$ ) and the slope of the virgin compression line, represented by the compression index ( $C_c$ ), vary with soil suction. For instance, over consolidation stress increases from 30 kPa to 176 kPa by varying suction from 0 to 400 kPa for the 1.0 m test depth.

The collapse potential ( $CP$ ) can be indirectly estimated quantifying the discontinuity between the saturated and unsaturated curves from Figure 9, in a similar way to the double tests proposed by Jennings & Knight (1975). There is a higher collapse potential ( $CP$ ) for the higher suction

values, which decreases with increasing depth (Figure 10). Therefore,  $CP$  is higher closer to the ground surface and for higher suction values.

Figure 11 shows an increase in the soil stiffness, represented by the oedometric modulus ( $M_d$ ), with increasing suction. It is also possible to observe in this figure that  $M_d$  values are relatively low up to about a net vertical stress equal 200 kPa and increase after that value. Soil that undergoes to a volume reduction due to collapse gets denser, which leads to an increase in the oedometric modulus with net vertical stress.

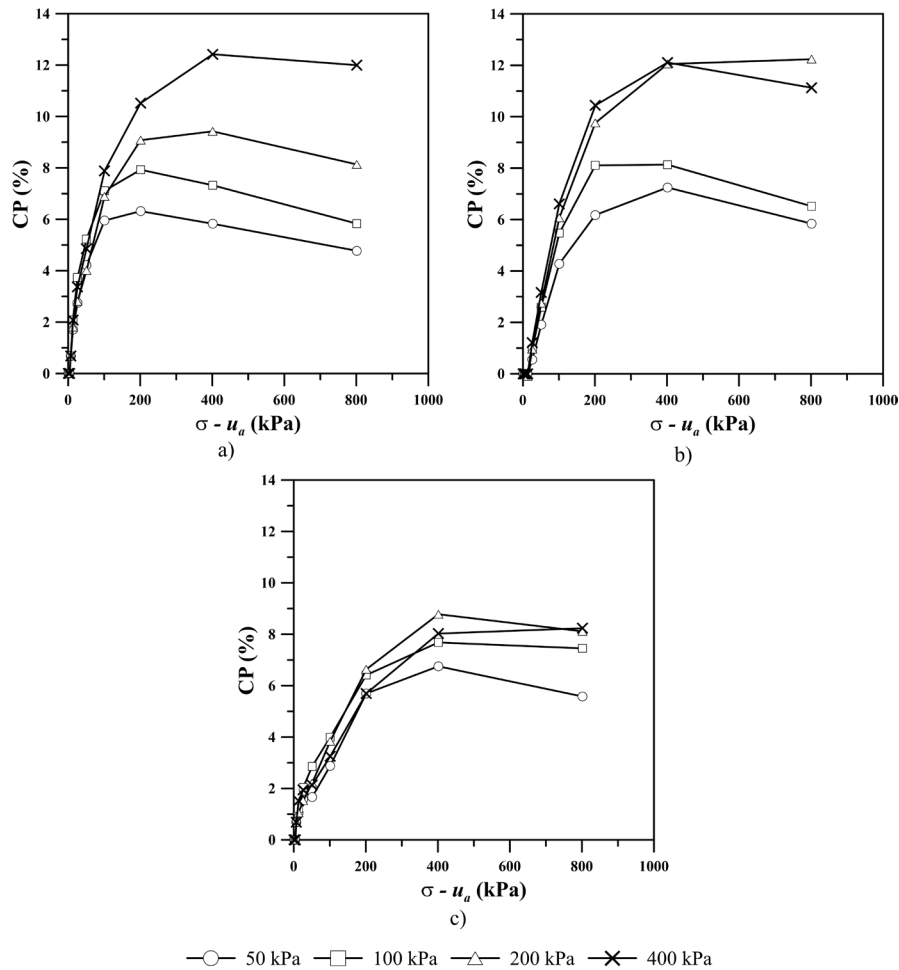


**Figure 10.** Collapse potential *versus* soil suction (50, 100, 200 and 400 kPa) for the different test depths: (a) 1.0; (b) 3.0; and (c) 5.0 m.

#### 4. The variation of geotechnical parameters with depth

Shear strength parameters ( $c$ ,  $\phi$ ), compressibility parameters ( $\sigma_p$ ,  $C_c$ ), maximum shear modulus ( $G_0$ ) and collapse potential ( $CP$ ) and their variation with soil suction along depth are summarized in Figure 12.

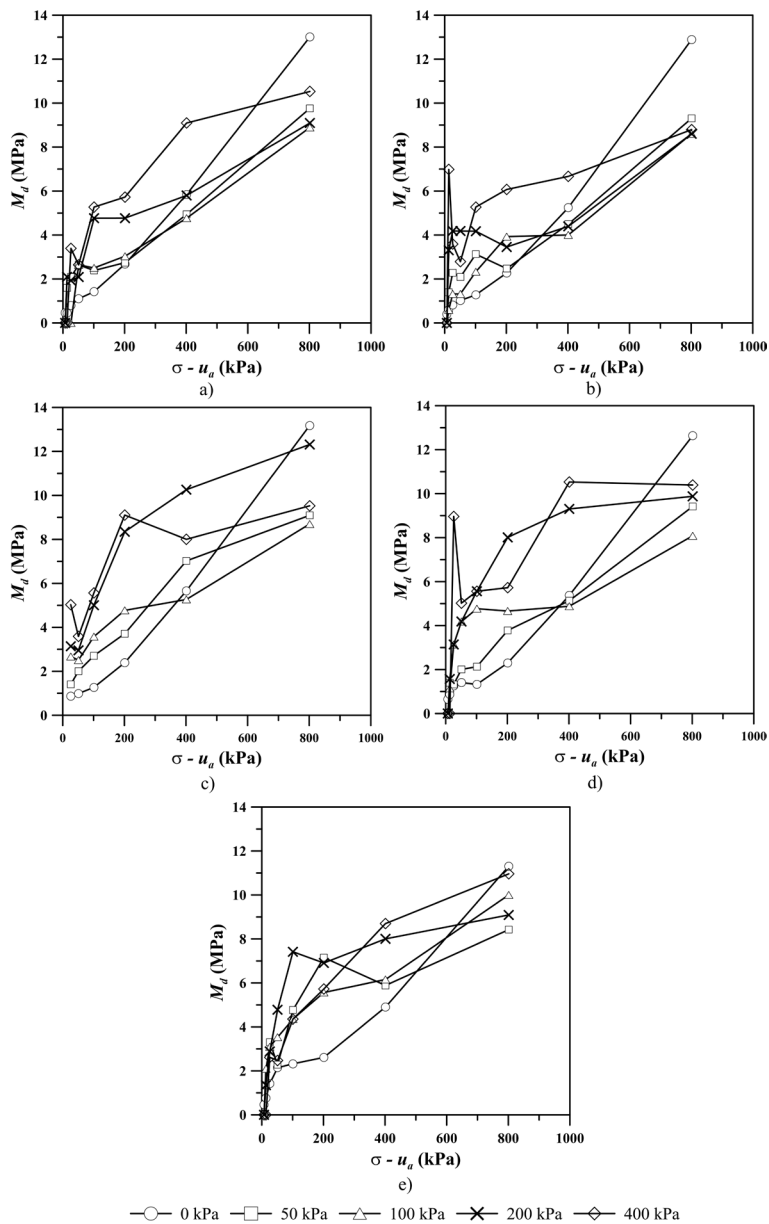
It can be observed from Figure 12 that the variation of the friction angle with suction is more pronounced for the 1.5 m depth than for 3.0 and 5.0 m depths. It can also be noted in this figure that the  $\phi$  angle is practically the same for 3.0 and 5.0 m depths and higher than the 1.5 m depth. This figure also shows that the cohesion intercept increases with suction and with depth.

The over consolidation stress ( $\sigma_p$ ) for the saturated condition is low and has little variation with depth, between 25 and 50 kPa (Figure 12). On the other hand, the  $\sigma_p$  increases with suction and with depth. The slope of the virgin compression line ( $C_c$ ) also varies with suction, but practically does not vary with depth. This figure also shows that the collapse potential ( $CP$ ) increases with soil suction and decreases with depth. The magnitude of collapsible behavior is higher in the upper portion of the soil

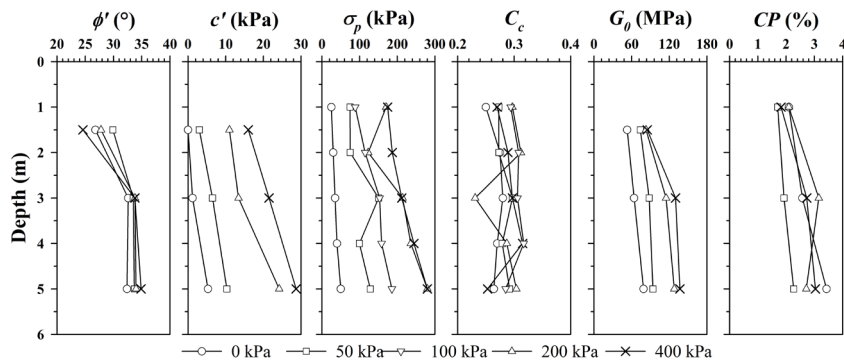
profile, and it increases with suction. In addition, the maximum shear modulus ( $G_0$ ) increases with soil suction and with depth. It is important to mention that the values of  $G_0$  and  $CP$  were determined from the estimated effective stress ( $\sigma'_v$ ) for the tested depths considering the unit weight of the studied soil.

Figure 12 also shows that the lower shear strength and the lower soil stiffness occurs at the 1.5 m depth, and these parameters slightly increase with depth for both the low and to the high suction values. It is also possible to observe that soil suction has a higher influence on cohesion intercept ( $c$ ) and on the over consolidation stress ( $\sigma_p$ ) than in friction angle ( $\phi$ ) and in compression index ( $C_c$ ).

Soil suction has greater influence on the geotechnical parameters in the active zone of the studied soil profile (Figure 12) than the physical index properties (grain size distribution, consistency limits, unit weight of solids and void ratio). The presented data highlight the importance of understanding the suction influence on the behavior of the active zone of the studied soil profile. Such aspect is important for shallow foundations design since variability caused by suction is more relevant than spatial variability at the study site.



**Figure 11.** Oedometric modulus ( $M_d$ ) versus the vertical stress at constant suction value for soil samples collected at (a) 1.0; (b) 2.0; (c) 3.0; (d) 4.0; and (e) 5.0 m depth.



**Figure 12.** Variation of cohesion intercept, internal friction angle, over consolidation stress, compression index, maximum shear modulus and collapse potential with suction along depth for the study site.

## 5. Conclusions

- Characterization tests, index properties, retention curves and the mechanical parameters determined along depth indicate that the profile is fairly homogeneous up to 5.0 m depth;
- Water retention curves showed a typical behavior of porous sandy soil, with low air entry value and accented desaturation curve. The bimodal format is due to the existence of two air entry values: the first because of the presence of macropores and the second because of the drainage of micropores of the soil aggregate fraction;
- There is little influence of depth on that soil shear strength up to 5.0 m depth. The higher contribution on strength parameters is due to soil suction, which increases the intercept cohesion with lower influence of the internal friction angle;
- Compressibility parameters, mainly the  $\sigma_p$ , are also more affect by suction than the depth. The increase on soil suction caused an increase in over consolidation stress ( $\sigma_p$ ) and changes in soil compression index ( $C_c$ ). The constrained modulus ( $M_d$ ) increases with increasing depth and soil suction;
- The  $G_0$  values tends to increase linearly with net confining stress and nonlinearly with soil suction for the three tested depths. The greater variation of  $G_0$  with suction was observed at 3.0 and 5.0 m depth samples;
- The soil has collapsible behavior with important collapse potential mainly under effect of higher suction values and closer to the ground surface;
- The geomechanical parameters of the studied soil are strongly influenced by suction and less influenced by depth and it must be incorporated to the practical design. In general, the presented test data show that the geotechnical parameters are more sensitive to soil suction than to the increase on depth in the active zone of the soil profile.

## Acknowledgements

The authors thank the São Paulo Research Foundation, FAPESP (Grant 2017/23174-5), the National Council for Scientific and Technological Development, CNPq (Grant 436478/2018-8) and the Coordination for the Improvement of Higher Education Personnel, CAPES, for supporting their research.

## Declaration of interest

The authors have no conflicts of interest to declare. All co-authors have observed and affirmed the contents of the paper and there is no financial interest to report.

## Authors' contributions

Jeferson Brito Fernandes: Conceptualization, Data curation, Visualization, Writing – original draft. Alfredo Lopes Saab: Conceptualization, Data curation, Methodology, Supervision, Validation, Writing – original draft. Breno Padovezi Rocha: Formal Analysis, Investigation, Methodology, Writing – review & editing. Paulo César Lodi: Experimental supervision, Validation, Writing – review & editing. Roger Augusto Rodrigues: Conceptualization, Experimental supervision, Methodology, Writing – review. Heraldo Luiz Giacheti: Conceptualization, Methodology, Supervision, Funding acquisition, Project administration, Writing – review.

## List of symbols

AEV	air entry value
a	fitting parameter
b	fitting parameter
B	pore-pressure coefficient
c	cohesion intercept
c'	effective cohesion intercept
$C_c$	compression index
CD	consolidated drained triaxial compression tests
CP	collapse potential
CPT	cone penetration test
CPTu	piezocone penetration test
E	void ratio
$E_{50}$	secant modulus in drained triaxial testing at 50 percent strength
f	fitting parameter
$f_s$	sleeve friction
g	fitting parameter
$G_0$	maximum shear modulus
$G_{0,sat}$	maximum shear modulus at the saturated condition
m	fitting parameter
$M_d$	oedometric modulus
n	fitting parameter
$q_c$	cone resistance
s	soil suction value
SM	silty sands
$R^2$	coefficient of determination
$V_s$	shear wave velocity
w	gravimetric moisture content
$w_L$	liquid limit
$w_p$	plastic limit
$\gamma_d$	dry unit weight
$\gamma_s$	unit weight of solids
$\rho$	soil bulk density
$\sigma_p$	over consolidation stress
$\sigma'_v$	effective stress
$\sigma - u_a$	net confining stress
$(\sigma_1 - \sigma_3)_{max}$	maximum deviatoric stress
t	shear stress
$\phi'$	friction angle
$\phi^b$	friction angle with respect to matric suction

## References

- ABNT NBR 9604. (1986). *Solo - Abertura de Poço e Trincheira de Inspeção em Solo, com Retirada de Amostras Deformadas e Indeformadas*. ABNT - Associação Brasileira de Normas Técnicas, Rio de Janeiro, RJ.
- Alonso, E.E., Gens, A., & Josa, A. (1990). A constitutive model for partially saturated soils. *Geotechnique*, 40(3), 405-430. <http://dx.doi.org/10.1680/geot.1990.40.3.405>.
- ASTM D2487-17. (2017). *Standard Practice for Classification of Soils for Engineering Purposes (Unified Soil Classification System)*. ASTM International, West Conshohocken, PA.
- Blight, G.E. (2003). The vadose zone soil-water balance and transpiration rates of vegetation. *Geotechnique*, 53(1), 55-64. <http://dx.doi.org/10.1680/geot.2003.53.1.55>.
- Chandler, R.J., & Gutierrez, C.I. (1986). The filter-paper method of suction measurement. *Geotechnique*, 36(2), 265-268. <http://dx.doi.org/10.1680/geot.1986.36.2.265>.
- Chandler, R.J., Crilly, M.S., & Montgomery-Smith, G. (1992). OA low-cost method of assessing clay desiccation for low-rise-buildings. *Proceedings of the Institution of Civil Engineers. Civil Engineering*, 92(2), 82-89. <http://dx.doi.org/10.1680/icien.1992.18771>.
- Cui, Y.J., Lu, Y.F., Delage, P., & Riffard, M. (2005). Field simulation of *in situ* water content and temperature changes due to ground-atmospheric interactions. *Geotechnique*, 55(7), 557-567. <http://dx.doi.org/10.1680/geot.2005.55.7.557>.
- De Mio, G. (2005). *Geological conditioning aspects for piezocone test interpretation for stratigraphical identification in geotechnical and geo-environmental site investigation* [Doctoral thesis, University of São Paulo]. University of São Paulo's repository (in Portuguese). Retrieved in January 9, 2022, from <https://teses.usp.br/teses/disponiveis/18/18132/tde-27042006-170324/pt-br.php>
- De Mio, G., & Giacheti, H.L. (2007). The use of piezocone tests for high-resolution stratigraphy of Quaternary sediment sequences in the Brazilian coast. *Anais da Academia Brasileira de Ciências*, 79(1), 153-170. <http://dx.doi.org/10.1590/S0001-37652007000100017>.
- Delage, P., Romero, E., & Tarantino, A. (July 2-4, 2008). Recent developments in the techniques of controlling and measuring suction in unsaturated soils. In *1st European Conference on Unsaturated Soils* (pp.33-52). Durham: Glasgow Universities.
- Dong, Y., & Lu, N. (2016). Correlation between small-strain shear modulus and suction stress in capillary regime under zero total stress conditions. *Journal of Geotechnical and Geoenvironmental Engineering*, 142(11), 04016056. [http://dx.doi.org/10.1061/\(ASCE\)GT.1943-5606.0001531](http://dx.doi.org/10.1061/(ASCE)GT.1943-5606.0001531).
- Dong, Y., Lu, N., & McCartney, J.S. (2018). Scaling shear modulus from small to finite strain for unsaturated soils. *Journal of Geotechnical and Geoenvironmental Engineering*, 144(2), 04017110. [http://dx.doi.org/10.1061/\(ASCE\)GT.1943-5606.0001819](http://dx.doi.org/10.1061/(ASCE)GT.1943-5606.0001819).
- Escario, V., & Sáez, J. (1986). The shear strength of partly saturated soils. *Geotechnique*, 36(3), 453-456. <http://dx.doi.org/10.1680/geot.1986.36.3.453>.
- Fernandes, J.B. (2016). *Shear strength and stiffness of an unsaturated soil by triaxial tests* [Master's dissertation, São Paulo State University]. São Paulo State University's repository (in Portuguese). Retrieved in January 9, 2022, from <https://repositorio.unesp.br/handle/11449/143473>
- Ferreira, C., Fonseca, A.V., & Nash, D.F.T. (2011). Shear wave velocities for sample quality assessment on a residual soil. *Soil and Foundation*, 51(4), 683-692. <http://dx.doi.org/10.3208/sandf.51.683>.
- Fredlund, D.G. (2006). Unsaturated soil mechanics in engineering practice. *Journal of Geotechnical and Geoenvironmental Engineering*, 132(3), 286-321. [http://dx.doi.org/10.1061/\(ASCE\)1090-0241\(2006\)132:3\(286\)](http://dx.doi.org/10.1061/(ASCE)1090-0241(2006)132:3(286)).
- Fredlund, D.G., & Morgenstern, N.R. (1977). Stress state variables for unsaturated soils. *Journal of the Geotechnical Engineering Division*, 103(5), 447-466. <http://dx.doi.org/10.1061/AJGEB6.0000423>.
- Fredlund, D.G., & Xing, A. (1994). Equations for the soil-water characteristic curve. *Canadian Geotechnical Journal*, 31(4), 521-532. <http://dx.doi.org/10.1139/t94-061>.
- Fredlund, D.G., Morgenstern, N.R., & Widger, R.A. (1978). The shear strength of unsaturated soils. *Canadian Geotechnical Journal*, 15(3), 313-321. <http://dx.doi.org/10.1139/t78-029>.
- Georgetti, G.B. (2014). *Stiffness and strength of a lateritic unsaturated soil* [Doctoral thesis, University of São Paulo]. University of São Paulo's repository (in Portuguese). Retrieved in January 9, 2022, from <https://teses.usp.br/teses/disponiveis/18/18132/tde-20032015-103943/en.php>
- Giacheti, H.L., Bezerra, R.C., Rocha, B.P., & Rodrigues, R.A. (2019). Seasonal influence on cone penetration test: an unsaturated soil site example. *Journal of Rock Mechanics and Geotechnical Engineering*, 11(2), 361-368. <http://dx.doi.org/10.1016/j.jrmge.2018.10.005>.
- Hardin, B.O., & Blandford, G.E. (1989). Elasticity of particulate materials. *Journal of Geotechnical Engineering*, 115(6), 788-805. [http://dx.doi.org/10.1061/\(ASCE\)0733-9410\(1989\)115:6\(788\)](http://dx.doi.org/10.1061/(ASCE)0733-9410(1989)115:6(788)).
- Hilf, J.W. (1956). *An investigation of pore-water pressure in compacted cohesive soils* [Doctoral thesis, University of Colorado]. United State Department of the Interior Bureau of Reclamation, Design and Construction Division, Denver, CO, USA.
- Ho, D.Y.F., & Fredlund, D.G. (January, 11-15, 1982). Increase in shear strength due to suction for two Hong Kong soils. In *ASCE Geotechnical Engineering Division Specialty Conference* (pp. 263-295). New York: American Society of Civil Engineers.
- Hoyos, L.R., Suescún-Florez, E.A., & Puppala, A.J. (2015). Stiffness of intermediate unsaturated soil from simultaneous suction-controlled resonant column and bender element

- testing. *Engineering Geology*, 188, 10-28. <http://dx.doi.org/10.1016/j.enggeo.2015.01.014>.
- Jamiolkowski, M. (2012). Role of geophysical testing in geotechnical site characterization. *Soils and Rocks*, 35(2), 117-137.
- Jennings, J.E., & Knight, K. (1975). A guide to construction on or with materials exhibiting additional settlement due to collapse of grain structure. In *6th Regional Conference for Africa on Soil Mechanics and Foundation Engineering* (pp. 99-105). Netherlands: A. A. Balkema.
- Khalili, N., & Khabbaz, M.H. (1998). A unique relationship for  $\chi$  for the determination of the shear strength of unsaturated soils. *Geotechnique*, 48(5), 681-687. <http://dx.doi.org/10.1680/geot.1998.48.5.681>.
- Lambe, T.W., & Whitman, R.V. (1976). *Soil mechanics*. Chichester: John Wiley & Sons.
- Leong, E.C., & Cheng, Z.Y. (2016). Effects of confining pressure and degree of saturation on wave velocities of soils. *International Journal of Geomechanics*, 16(6), [http://dx.doi.org/10.1061/\(ASCE\)GM.1943-5622.0000727](http://dx.doi.org/10.1061/(ASCE)GM.1943-5622.0000727).
- Leong, E.C., Cahyadi, J., & Rahardjo, H. (2006). Stiffness of a compacted residual soil. In *Unsaturated Soils 2006* (pp. 1169-1180). Reston. American Society of Civil Engineers. [https://doi.org/10.1061/40802\(189\)95](https://doi.org/10.1061/40802(189)95).
- Mancuso, C., Vassallo, R., & D'Onofrio, A. (2002). Small strain behavior of a silty sand in controlled-suction resonant column - torsional shear tests. *Canadian Geotechnical Journal*, 39(1), 22-31. <http://dx.doi.org/10.1139/t01-076>.
- Marinho, F., & Oliveira, O. (2006). The filter paper method revisited. *Geotechnical Testing Journal*, 29(3), 14125. <http://dx.doi.org/10.1520/GTJ14125>.
- Nyunt, T.T., Leong, E.C., & Rahardjo, H. (2011). Strength and small-strain stiffness characteristics of unsaturated sand. *Geotechnical Testing Journal*, 34(5), 103589. <http://dx.doi.org/10.1520/GTJ103589>.
- Ray, R.L., Jacobs, J.M., & Alba, P. (2010). Impacts of unsaturated zone soil moisture and groundwater table on slope instability. *Journal of Geotechnical and Geoenvironmental Engineering*, 136(10), 1448-1458. [http://dx.doi.org/10.1061/\(ASCE\)GT.1943-5606.0000357](http://dx.doi.org/10.1061/(ASCE)GT.1943-5606.0000357).
- Rocha, B.P., Rodrigues, A.R.C., Rodrigues, R.A., & Giacheti, H.L. (2022). Using a seismic dilatometer to identify collapsible soils. *International Journal of Civil Engineering*, 20, 857-867. <http://dx.doi.org/10.1007/s40999-021-00687-9>.
- Rocha, B.P., Rodrigues, R.A., & Giacheti, H.L. (2021). The flat dilatometer test in an unsaturated tropical soil site. *Geotechnical and Geological Engineering*, 39(8), 5957-5969. <http://dx.doi.org/10.1007/s10706-021-01849-1>.
- Röhm, S.A., & Vilar, O.M. (September 6-8, 1995). Shear strength of an unsaturated sandy soil. In *Proceedings of the First International Conference on Unsaturated Soils* (pp. 189-193). Netherlands: A. A. Balkema.
- Sánchez, M., Wang, D., Briaud, J.L., & Douglas, C. (2014). Typical geomechanical problems associated with railroads on shrink-swell soils. *Transportation Geotechnics*, 1(4), 257-274. <http://dx.doi.org/10.1016/j.trgeot.2014.07.002>.
- Silva, N.M., Rocha, B.P., & Giacheti, H.L. (2019). Prediction of load-settlement curves by the DMT in an unsaturated tropical soil site. *Soils and Rocks*, 42(3), 351-361. <http://dx.doi.org/10.28927/SR.423351>.
- Skempton, A.W., & Jones, O.T. (1944). Notes on the compressibility of clays. *Quarterly Journal of the Geological Society*, 100(1-4), 119-135. <http://dx.doi.org/10.1144/GSL.JGS.1944.100.01-04.08>.
- Sun, D., Sheng, D., & Xu, Y. (2007). Collapse behaviour of unsaturated compacted soil with different initial densities. *Canadian Geotechnical Journal*, 44(6), 673-686. <http://dx.doi.org/10.1139/t07-023>.
- Takkabutr, P. (2006). *Experimental investigations on small-strain stiffness properties of partially saturated soils via resonant column and bender element testing* (Doctoral thesis). University of Texas at Arlington.
- Toll, D.G. (1990). A framework for unsaturated soil behaviour. *Geotechnique*, 40(1), 31-44. <http://dx.doi.org/10.1680/geot.1990.40.1.31>.
- Tsiampousi, A., Zdravkovic, L., & Potts, D.M. (2017). Numerical study of the effect of soil-atmosphere interaction on the stability and serviceability of cut slopes in London clay. *Canadian Geotechnical Journal*, 54(3), 405-418. <http://dx.doi.org/10.1139/cgj-2016-0319>.
- van Genuchten, M. (1980). A Closed-form equation for predicting the hydraulic conductivity of unsaturated soils. *Soil Science Society of America Journal*, 44(5), 892-898. <http://dx.doi.org/10.2136/sssaj1980.03615995004400050002x>.
- Vanapalli, S.K., Fredlund, D.G., Pufahl, D.E., & Clifton, A.W. (1996). Model for the prediction of shear strength with respect to soil suction. *Canadian Geotechnical Journal*, 33(3), 379-392. <http://dx.doi.org/10.1139/t96-060>.
- Vilar, O.M. (2006). A simplified procedure to estimate the shear strength envelope of unsaturated soils. *Canadian Geotechnical Journal*, 43(10), 1088-1095. <http://dx.doi.org/10.1139/t06-055>.
- Vilar, O.M., & Rodrigues, R.A. (2011). Collapse behavior of soil in a Brazilian region affected by a rising water table. *Canadian Geotechnical Journal*, 48(2), 226-233. <http://dx.doi.org/10.1139/T10-065>.
- Zhang, J., Huang, H.W., Zhang, L.M., Zhu, H.H., & Shi, B. (2014). Probabilistic prediction of rainfall-induced slope failure using a mechanics-based model. *Engineering Geology*, 168, 129-140. <http://dx.doi.org/10.1016/j.enggeo.2013.11.005>.
- Zhang, X. (2016). Limitations of suction-controlled triaxial tests in the characterization of unsaturated soils. *International Journal for Numerical and Analytical Methods in Geomechanics*, 40(2), 269-296. <http://dx.doi.org/10.1002/nag.2401>.